Small-Angle Scattering Investigations of Poly(ε-caprolactone)/Polycarbonate Blends. 2. Small-Angle X-ray and Light Scattering Study of Semicrystalline/Semicrystalline and Semicrystalline/Amorphous Blend Morphologies

Y. Wilson Cheung*,† and Richard S. Stein*

Department of Polymer Science and Engineering, University of Massachusetts, Amherst, Massachusetts 01003

J. S. Lin and George D. Wignall

Oak Ridge National Laboratory, Oak Ridge, Tennessee 37831

Received September 7, 1993; Revised Manuscript Received January 14, 1994®

ABSTRACT: Crystalline morphologies of poly(ε-caprolactone) (PCL) and polycarbonate (PC) blends were probed with small-angle X-ray scattering (SAXS) and small-angle light scattering (SALS). Quantitative SAXS analysis suggested that random mixing of PCL and PC lamellae occurred in the semicrystalline/semicrystalline state. Two distinct regions of incorporation were identified in the semicrystalline/amorphous state. It was found that PCL was rejected from the PC interlamellar region in the PCL-rich blends. In contrast, PCL was incorporated into the amorphous phase between the crystalline lamellae in the PC-rich blends. This transition from interlamellar exclusion to interlamellar inclusion may be related to the glass transition temperatures or the mobility of the blends. It is proposed that the mode of incorporation or exclusion is governed by the competition between entropy and diffusion. Additionally, SALS coupled with optical microscopy indicated that PC is an effective nucleating agent for PCL crystallization as manifested by the reduction of PCL spherulitic size with the addition of PC.

Introduction

Depending on the composition and the thermal and processing conditions, poly(ε-caprolactone) (PCL)/polycarbonate (PC) blends can exhibit a wide spectrum of morphologies ranging from a single phase to a highly complex three-phase material. The phase behavior and the miscibility of this blend system are critically examined in a separate paper.[1] The PCL-rich blends (containing >50% PCL) are semicrystalline/semicrystalline at room temperature as revealed by differential scanning calorimetry (DSC) and wide-angle X-ray scattering (WAXS). These measurements indicated that there exists no evidence for cocrystallization as the unit cell geometry and parameters for PCL (orthorhombic) and PC (monoclinic) are very different.[2,3] The PCL-rich blends become semicrystalline/amorphous materials at temperatures above the melting point of PCL. On the basis of thermal analysis results,[4,5] this blend system is miscible in the amorphous phase over the entire composition range as evidenced by the presence of a single glass transition temperature.

Elucidation of the blend morphologies is of paramount importance in understanding the extent of polymer–polymer interaction and the physical properties. The interplay between kinetics and thermodynamics invariably determines the blend morphologies. The semicrystalline/amorphous state of PCL/deuterated PC (d-PC) blends as revealed by small-angle neutron scattering (SANS) was discussed in the first part of this series of investigations.[6] On the basis of the modified Debye–Bueche analysis, the morphology of PCL/d-PC blends may be described by a model composed of a d-PC crystalline phase dispersed in a matrix amorphous phase consisting of local clusters ~30 Å in size. A more detailed analysis of the SAXS results will be explored in this paper. The main focus of this part of the investigations is to examine the blend morphologies, at both the lamellar and spherulitic levels, in both the semicrystalline/semicrystalline and semicrystalline/amorphous states. SAXS is employed to unravel the lamellar organization of both PCL and PC. Correlation function analysis, absolute invariant calculation, and Porod analysis will be used to determine the characteristic morphological parameters including the crystal- and amorphous-phase thicknesses and the transition layer thickness. Small-angle light scattering (SALS) coupled with polarized optical microscopy is used to probe the spherulitic structure.

Depending on the polymer–polymer specific interactions and the cooperative diffusion coefficient, a wide spectrum of morphologies may be found in semicrystalline/amorphous blends. The amorphous component in such a blend system can reside between the crystalline lamellae (interlamellar), can be incorporated within the spherulites (interfibrillar), or can even be rejected from the spherulites (interspherulitic). The interlamellar case has been observed in blends of PCL with poly(vinyl chloride) (PVC),[7] poly(vinylidene fluoride) (PVF_2) with poly(methyl methacrylate) (PMMA),[8] and poly(ethylene oxide) (PEO) with PMMA.[9] The interfibrillar case is found in blends of isotactic polystyrene and atactic polystyrene.[10] The last mode of incorporation has been demonstrated in blends of high and low molecular weight PEO.[11]

In the case of semicrystalline/semicrystalline blends, there can exist even more possible structures and much more complex morphologies. Blends of random copolymers of vinylidene fluoride/trifluoroethylene (VF_2/FE_3) of different compositions were found to undergo cocrystallization.[12] More recently, blends of linear low-density polyethylene (LLDPE) and high-density polyethylene (HDPE) were also observed to crystallize within a single lattice.[13] Since both PCL and PC can crystallize in the PCL-rich blends, the PCL/PC system may be classified as a semicrystalline/semicrystalline blend. The necessary

† Present address: Dow Chemical Co., Midland, MI 48674.

® Abstract published in *Advance ACS Abstracts*, March 15, 1994.

0024-9297/94/2227-2520$04.50/0

conditions for cocrystallization are based on (1) miscibility in the melt, (2) similarity in the crystalline structure of the individual polymers, and (3) a nearly identical crystallization window. As mentioned before, no cocrystallization can occur between PCL and PC as the lattice parameters for the two polymers are fundamentally different.[2,3] In the semicrystalline/semicrystalline state, the PCL and PC lamellae may either order in blocks rich in one population of lamellae (segregated arrangement) or mix in a random fashion where the two different types of lamellae are homogeneously dispersed in the amorphous phase. Efforts will be made to discriminate these two modes of lamellar arrangement.

In addition to the composition and temperature, the effects of blend preparation and thermal history on the morphology will be examined. Blends are normally prepared by melting blending, solution casting from a common solvent, or solution blending followed by precipitation where the blend is recovered by precipitating the solution in a nonsolvent. Three different types of samples will be discussed: (1) as-precipitated (AP) blends, (2) quenched (Q) blends by first heating the AP blends to a temperature above the melting point of PC and then quenching the samples to room temperature, and (3) solution-cast (SC) blends. Both the PCL and PC crystallinities are strongly dependent on the preparation procedure, and consequently the lamellar arrangements may be different. Attempts will be made to decouple the effects of the amorphous and crystalline components on the lamellar and spherulitic organizations.

Experimental Section

The deuterated PC was synthesized by solution polymerization of deuterated bisphenol with phosgene at 0 °C in methylene chloride.[6] Both PCL and nondeuterated PC were obtained from Scientific Polymer Products. The molecular weights of the individual polymers are identical to those found in ref 6. Homogeneous methylene chloride solutions containing ~5 wt % polymer were first prepared, and blend samples were recovered either by precipitating the solution in about a tenfold excess of methanol or casting the solution on an aluminum surface. Blends were first dried under ambient conditions overnight and then dried in a vacuum oven at 90 °C for 2 days to ensure complete removal of residual solvent. Quenched samples were prepared by heating the samples to 250 °C for 3 min and rapidly transferred to room temperature. Scattering samples were compression molded typically at T_g + 50 °C under vacuum. Samples were then transferred to a metal surface and quenched to room temperature. The sample disk was ~1 mm thick and 15 mm in diameter.

Thermal transitions were measured with a DuPont 10 differential scanning calorimeter (DSC) at a heating rate of 20 °C/min. The glass transition temperatures were obtained from the second heating scan and determined from the midpoint of the change in the heat capacity. Melting points were recorded from the peak temperatures of the melting endotherms measured from the first heating scan. On the basis of the values for the heat of fusion for 100% crystalline PC[14] (35.3 cal/g) and PCL[15] (32.4 cal/g), the degree of crystallinity of both PCL and PC was calculated from the melting endotherm and normalized with respect to the composition of each component in the blend.

SAXS experiments were conducted at the Oak Ridge National Laboratory (ORNL) in Tennessee. Measurements were performed on the ORNL 10-m spectrometer[16] operating at an accelerating voltage of 40 kV and a current of 100 mA at both room temperature and 75 °C. The instrument was operated with a sample–detector distance of 5.13 m using Cu Kα radiation (λ = 1.54 Å) and a 20 × 20 cm^2 area detector with cell (element) size ~3 mm. Corrections were made for instrumental backgrounds and detector efficiency (via an Fe^{55} standard which emits γ-rays isotropically) on a cell-by-cell basis prior to radial averaging to yield a q range of 0.005–0.1 Å^{-1}, where $q = (4\pi/\lambda)\sin(\theta/2)$, λ = X-ray wavelength, and θ = scattering angle. The scattering profiles were corrected for sample absorption and incident X-ray fluctuations. The net intensities were converted to an absolute differential cross section per unit sample volume (in units of cm^{-1}) by comparison with precalibrated secondary standards.[17] Thermal density fluctuation scattering was estimated by measuring the SAXS at high scattering vectors, $0.019 < q < 0.47$ Å^{-1}, and eliminated by evaluating the slope of the Iq^4 versus q^4 plot.[9]

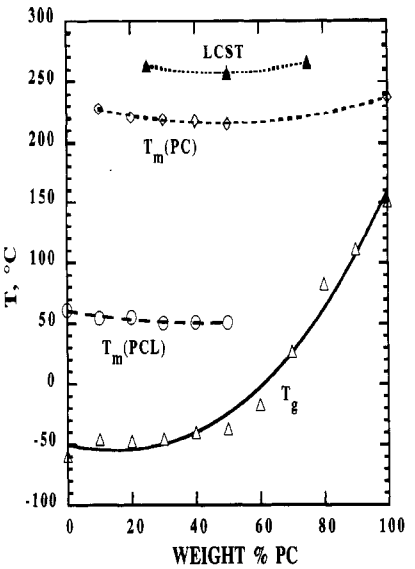

Figure 1. Phase transitions were measured at 20 °C/min with the exception of the LCST, which was measured at 4 °C/min. T_g = glass transition temperature, T_m = melting temperature, and LCST = lower critical solution temperature.

The small-angle light-scattering (SALS) patterns were recorded either by a film or by an optical multichannel analyzer with a laser light source of 6328-Å wavelength under horizontal–vertical (H_v) polarization conditions. A Zeiss optical microscope equipped with a cross polarizer was used to image the spherulites directly and to complement the SALS observations.

Results and Discussion

Differential Scanning Calorimetry. The phase transitions measured at 20 °C/min for the nondeuterated PC/PCL blends are shown in Figure 1. In addition to the multiple melting transitions, this system exhibits a lower critical solution temperature (LCST), where the two polymers undergo phase separation, close to the decomposition temperatures. The phase transitions and the crystallinities for the deuterated PC/PCL blends prepared from solution casting have been discussed in the first part of this investigation.[6] In agreement with previous studies,[4,5] this blend system exhibits a single glass transition temperature over the entire composition range, thereby suggesting miscibility in the amorphous phase. However, results obtained from the recent (SANS) study[6] in the semicrystalline/amorphous state suggested local clustering in the size range of ~30 Å in the amorphous phase. This kind of microheterogeneity may be related to and could result from crystallization-induced phase separation. Due to the plasticization of PC by PCL, both PC and PCL in the PCL-rich blends readily undergo crystallizaiton at room temperature. Due to the presence of crystallinities, the composition of the amorphous phase is different from the overall blend composition. Thus, the measured T_g shown in Figure 1 only reflects that of the semicrystalline samples as truly amorphous samples cannot be prepared due to the thermodynamics of this blend system. Figure 1 indicates that blends containing >30% PCL have glass transition temperatures below room temperature, which results in a significant widening of the crystallization

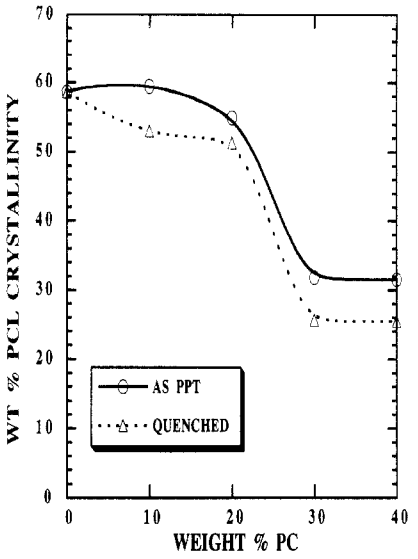

Figure 2. Normalized weight percent PCL crystallinity for as-precipitated (AP) and quenched (Q) PCL/PC blends.

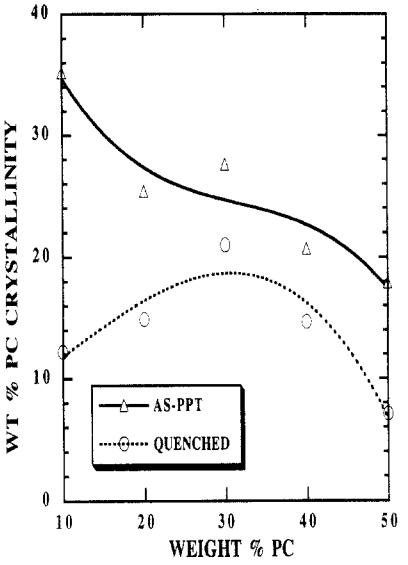

Figure 3. Normalized weight percent PC crystallinity for as-precipitated (AP) and quenched (Q) PCL/PC blends.

window for PC. Therefore, PCL is a very effective macromolecular plasticizer for PC.

The PCL and PC crystallinities for both the as-precipitated (AP) and quenched (Q) blends, normalized with respect to the composition of each component, as a function of composition are plotted in Figures 2 and 3, respectively. The AP blends always have higher PC crystallinity than the corresponding Q blends. The lower crystallinity found in the Q blends resulted from the destruction of the annealing effects by quenching the samples from above the melting point of PC. Effectively, the PC crystallinity found in the Q samples may be viewed as the "quasi-equilibrium" crystallinity at room temperature whereas the higher PC crystallinity measured from the AP samples is closer to the "equilibrium" crystallinity at 90 °C. In contrast, the PCL crystallinity is not strongly affected by sample preparation. Interestingly, the PCL crystallinity showed a marked reduction at ~30% PC composition. This phenomenon is explored further in a separate study.[1]

Small-Angle X-ray Scattering. I. SAXS Analysis. SAXS is a very powerful morphological tool for studying the detailed lamellar organization of semicrystalline polymers. It is well known that the contrast mechanism

Table 1. Electron Density (ρ_e) and Mass Density (d) Electron Density Difference ($\Delta\rho_e$) for PCL and PC[a]

polymer	$\rho_e \times 10^{-9}$ (cm^{-2})	d_A (g/cm^3)	d_X (g/cm^3)	$(\Delta\rho_e)^2 \times 10^{-20}$ (cm^{-4})
PCL	91.72d	1.090	1.185	1.118
PC	88.97d	1.196	1.315	0.760

[a] A = amorphous; X = crystalline; $\Delta\rho_e = \rho_{eA} - \rho_{eX}$.

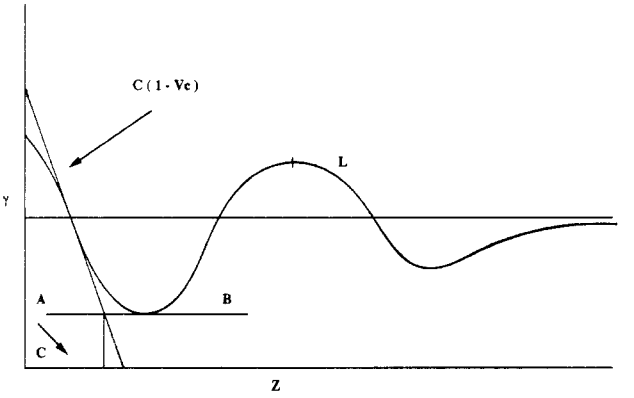

Figure 4. Schematic drawing of a correlation function with L = long period, C = crystalline-phase thickness, and V_c = the volume crystallinity. The x intercept yields $C(1 - V_c)$ and the amorphous-phase thickness $A = L - C$.

for SAXS is based on the electron density difference between the crystalline and amorphous regions. The mass density, the electron densities for PC and PCL, and the electron density difference between the crystalline and the amorphous regions for PCL and PC are displayed in Table 1. It can be seen that the contrast for PC is ~1.5 times greater than that for PCL. This fact is critical to the analysis of the absolute scattering cross section of the blends to be described later.

Traditionally, three approaches are often used to analyze the SAXS profiles: (1) calculation of the long period or the interlamellar spacing directly from the scattering curve, (2) computation of the electron density correlation function[18-20] from which the amorphous- and crystal-phase thicknesses may be obtained, and (3) fitting of the scattering profiles to morphological models.[21-23] The first two methods will be used to evaluate the various morphological parameters. The long period is calculated from the equation $L = 2\pi/q^*$, where q^* is the peak value found in the Lorentz-corrected ($q^2I(q)$ versus q) plot. The normalized one-dimensional correlation can be evaluated from the scattered intensity $I(q)$ by the following equation:[19]

$$\gamma(z) = \frac{1}{\gamma(0)}\int_0^\infty q^2 I(q)\cos(qz)\,dq \qquad (1)$$

where z is along the direction from which the electron density distribution is measured. Since the experimentally accessible q range is finite, it is necessary to extend the data to both lower and higher q values. Linear extrapolation is used to extend the data from the smallest measured q value to zero. Large q values could be damped to infinite q value by using a Porod-type (q^{-4} decay) model.[19] A schematic depiction of a correlation function is shown in Figure 4.

Peak width measured at half-height of the Lorentz-corrected SAXS profiles will be used to assess the heterogeneity of the lamellar distribution. Porod analysis will be performed to determine the transition zone width between regions of different electron densities. In addition to the other corrections, the thermal density fluctuations

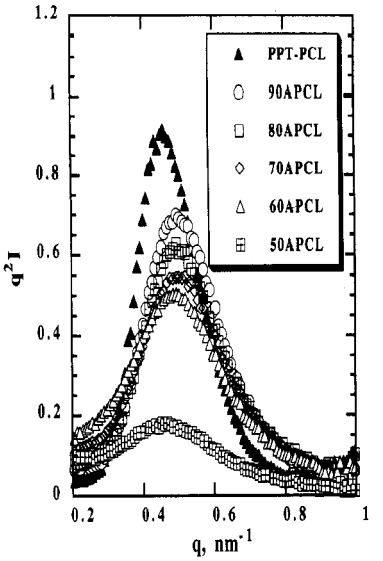

Figure 5. Lorentz-corrected SAXS curves recorded at room temperature for as-precipitated PCL-rich blends.

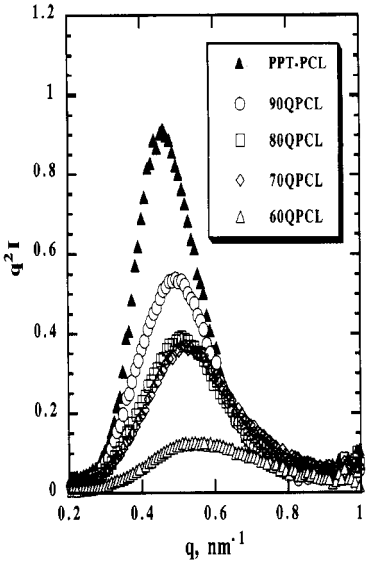

Figure 6. Lorentz-corrected SAXS profiles recorded at room temperature for quenched PCL-rich blends.

must be subtracted from the background scattering. Based on the Porod law,[24,25] the thermal fluctuations and the interface thickness can be expressed as

$$q^4I(q) = K_pH^2(q) + I_{fl}q^4 \tag{2}$$

where $H^2(q) = \exp(-\sigma^2q^2)$ is a Gaussian smoothing function, which accounts for the negative deviations from the Porod law due to the presence of an interface, with σ as the standard deviation. The interfacial thickness E is related to σ by the equation $E = 12^{1/2}\sigma$. I_{fl} is the background scattering due to the thermal density fluctuations and can be estimated from the slope of a plot of $q^4I(q)$ versus q^4 at large scattering vectors. Similarly, the interfacial thickness can be estimated from the slope of a plot of $\ln\{[I(q) - I_{fl}]q^4\}$ versus q^2. Finally, the total integrated intensity or the invariant Q, defined below,

$$Q = \frac{1}{2\pi^2}\int_0^\infty I(q)q^2\,dq \tag{3}$$

measured experimentally will be compared to the model calculation. For an ideal two-phase system, the invariant is given by

$$Q = 2\pi^2\phi_1\phi_2(\rho_1 - \rho_2)^2 \tag{4}$$

where ϕ is the volume fraction and ρ is the electron density. This definition may be generalized to a system containing an arbitrary number of phases as the following:[27]

$$Q = 2\pi^2\sum_{i\neq j}\phi_i\phi_j(\rho_i - \rho_j)^2 \tag{5}$$

II. Structure of Semicrystalline/Semicrystalline Blends. As described before, the PCL-rich blends at room temperature contained both PCL and PC crystals as evidenced by DSC and WAXS. A series of Lorentz-corrected SAXS profiles for the AP and Q blends are shown in Figures 5 and 6, respectively. On the basis of Figure 3, the AP samples have higher PC crystallinity than the Q samples. The SAXS profiles clearly indicate that the peak intensity and the total scattered intensity for the AP blends were higher than those for the corresponding Q blends due to the higher electron density difference for PC. From the peak position, the long period L or the interlamellar spacing can be obtained. Figure 7 shows a

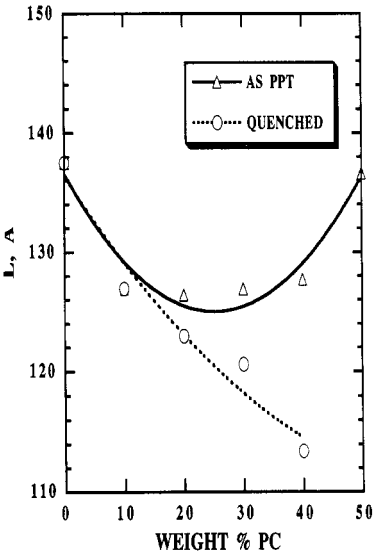

Figure 7. Long period measured at room temperature (in the semicrystalline/semicrystalline state) for as-precipitated and quenched blends.

plot of the long period as a function of composition for both AP and Q blends. A cursory examination of this plot indicates that the long period for the blends was always smaller than that for the pure PCL. For the AP blends, the long period was almost independent of composition. In the case of the Q blends, L decreased with the addition of PC. Effectively, the long period was dependent not only on the PC composition but also on the PC crystallinity.

Since these blends were semicrystalline/semicrystalline, the long period measured was assumed to be the average interlamellar spacing between the PCL and PC lamellae. The observation that the SAXS profiles for all the blends exhibited a single peak could suggest random mixing between the PC and PCL lamellae as a segregated arrangement should give rise to two peaks or at least a shoulder in the SAXS. This hypothesis is further supported by the finding that the PC long periods measured at 75 °C (above the melting point of PCL) shown in Figure 8 were different from and larger than those obtained at room temperature. Random mixing of the smaller PCL lamellae with the larger PC lamellae resulted in a depression of the observed long period found in the semicrystalline/semicrystalline state relative to that mea-

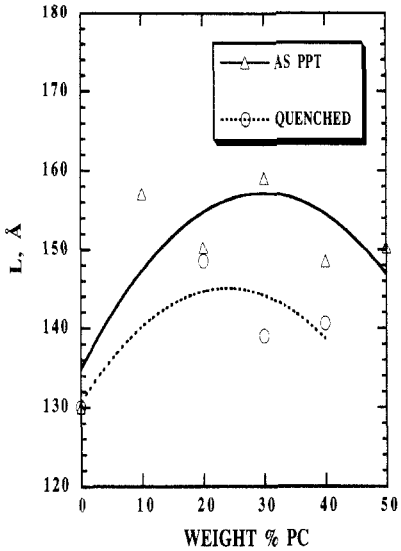

Figure 8. Long period measured at 75 °C (in the semicrystalline/amorphous state) for as-precipitated and quenched blends.

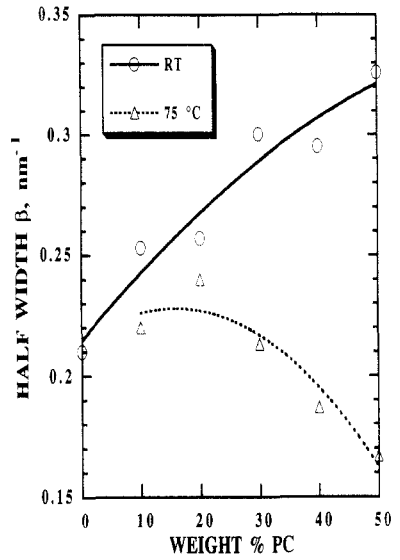

Figure 9. Peak width at half-height of the Lorentz-corrected SAXS profiles for as-precipitated blends measured at room temperature and 75 °C.

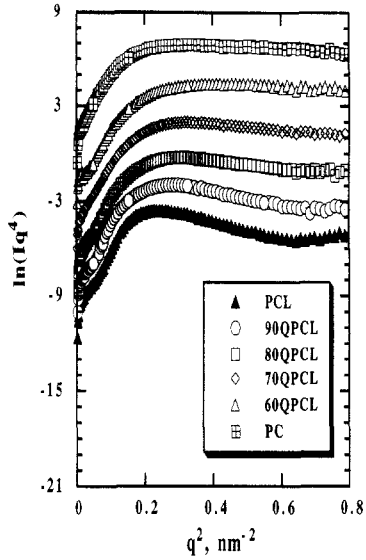

Figure 10. Porod plots (at room temperature) for pure PCL, quenched PCL-rich blends, and pure PC.

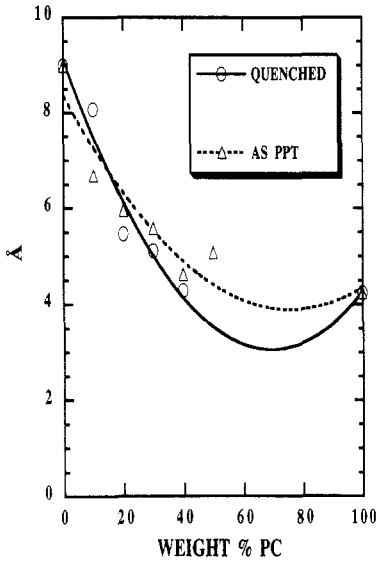

Figure 11. Interfacial thickness for quenched and as-precipitated blends measured at room temperature.

sured in the semicrystalline/amorphous state. This random mixing model can also explain the differences in the long period composition dependence between the AP and Q blends. The relative invariant of the long period with composition for the AP blends reflected the large contribution of the PC lamellar scattering, due to the higher PC crystallinity, to the SAXS pattern as the PC long period (measured in the semicrystalline/amorphous state) was fairly independent of composition as shown in Figure 8. The PCL long period in the PCL-rich blends cannot be isolated as the SAXS measured at room temperature is a superposition of both PCL and PC lamellar scattering. Therefore, the SAXS profiles recorded at room temperature could be interpreted as resulted from the scattering of entitites consisting of both PCL and PC lamellae.

Peak width, β, measured at half-height of the Lorentz-corrected SAXS profiles can be used as a measure of the homogeneity of the lamellar distribution. Figure 9 shows a plot of the peak width as a function of composition for the AP blends. It is observed that β increased with the addition of PC in the semicrystalline/semicrystalline state. In contrast, β decreased with increasing PC in the semicrystalline/amorphous state. Furthermore, β measured in the semicrystalline/semicrystalline state was consistently larger than that obtained in the semicrystalline/amorphous state. In other words, the lamellar distribution was narrower in the semicrystalline/amorphous state as the PCL lamellae were destroyed and did not contribute to the overall SAXS pattern. The larger lamellar heterogeneity found in the semicrystalline/semicrystalline blends further supports the random mixing model. The lamellar peak broadening reflects an increase in the heterogeneity of the lamellar distribution which results from the random mixing of the PCL and PC lamellae.

Porod analysis is commonly used to estimate the width of the transition zone. The slope of a plot of $\ln\{[I(q) - I_{fl}]q^4\}$ versus q^2 is proportional to the width of the interfacial thickness as described earlier. A series of Porod plots for the quenched blends are shown in Figure 10, and the corresponding interfacial thickness as a function of composition for Q and AP blends is plotted in Figure 11. Due to the statistical scatter in the intensity data and the difficulty of separating the effects of density fluctuations within the phases, the errors associated with the absolute value of the interfacial thickness could be significant.[28] Therefore, emphasis is directed at the composition dependence of the interfacial thickness rather than its

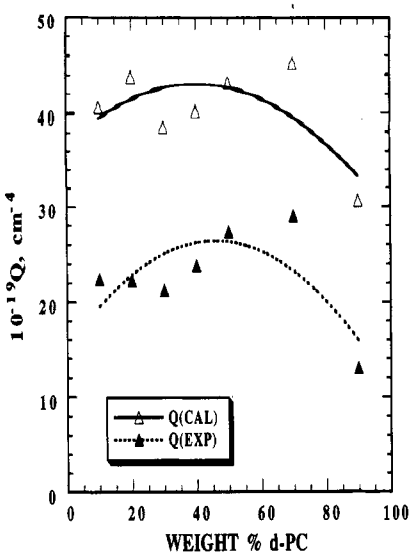

Figure 12. Comparison of the experimentally measured absolute invariant (EXP) to the calculated invariant (CAL) in the semicrystalline/semicrystalline state.

absolute value. A monotonic decrease in the interfacial width was found with increasing PC. Similar trends were also observed in the solution-cast blends. Interestingly, the interfacial width of the blends was intermediate of the two homopolymers. This finding provides an additional support for the random mixing model in which both PCL and PC lamellae scatter as a single entity. The PC character of the blends became more prominent as the interfacial width approached that of the pure PC with increasing PC composition and increasing PC crystallinity in the blends.

The total integrated scattered intensity or the invariant is directly related to the mean square fluctuation of electron density and can be calculated according to eq 5. At room temperature the PCL-rich blends consist of a PCL crystalline phase, a PC crystalline phase, and an amorphous phase. To a first order of approximation, the invariant may be calculated from the following "pseudo-two-phase" model

$$Q = 2\pi^2[\phi_1\phi_2(\rho_1-\rho_2)^2 + \phi_1\phi_3(\rho_1-\rho_3)^2 + \phi_1\phi_4(\rho_1-\rho_4)^2 + \phi_2\phi_3(\rho_2-\rho_3)^2 + \phi_2\phi_4(\rho_2-\rho_4)^2 + \phi_3\phi_4(\rho_3-\rho_4)^2] \quad (6)$$

where ϕ is the volume fraction, ρ is the electron density, and subscript 1 denotes crystalline PCL, subscript 2 amorphous PCL, subscript 3 crystalline PC, and subscript 4 amorphous PC phase. The values for the volume fraction for the various phases were derived from the DSC measurements and the overall blend composition. Figure 12 shows a comparison between the experimentally measured invariants and the calculated values for the solution-cast (d-PC/PCL) blends. The model calculation exhibits the same composition dependence as the experimental invariant. Moreover, the calculated values differed from the experimental values by ~50%. Invariably the calculated invariant was greater than the measured invariant. The discrepancy between the measured and the calculated invariant may be attributed to (1) inadequacy of the model, (2) a limited experimentally accessible q range, and (3) the existence of the transition zone, which would reduce the electron density difference between the phase and thus decrease the scattering contrast. The simple model used in the calculation neglects the presence of the crystal–amorphous interface.[29] Uncertainties associated with the crystallinity measurement and the presence of microvoids also could affect the scattering

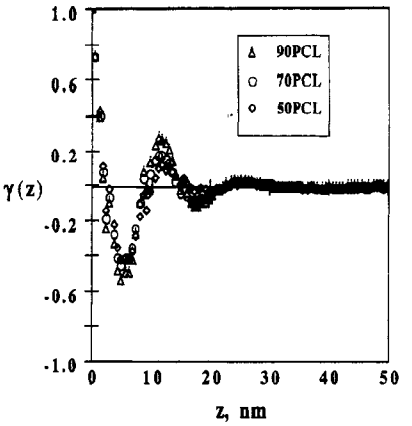

Figure 13. Correlation function evaluated at room temperature for the as-precipitated PCL-rich blends.

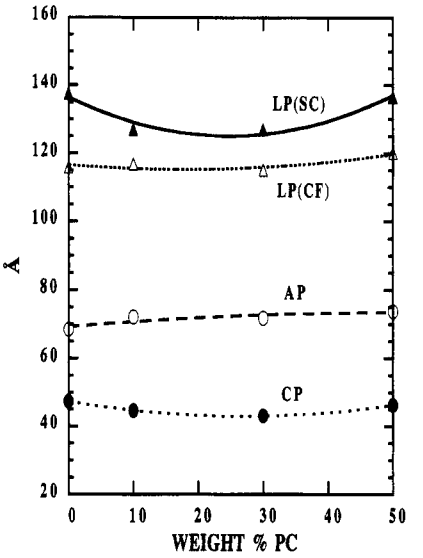

Figure 14. Correlation function results for the as-precipitated blends measured at room temperature. LP(SC) = long period directly calculated from SAXS, LP(CF) = long period obtained from the correlation function, AP = amorphous-phase thickness, and CP = crystal-phase thickness.

intensity and consequently the invariant. Additionally, the measured invariant represents an integration of the scattered intensity over a finite q range, which could easily lead to a lower value compared to the calculation. Extrapolations to both lower and higher q ranges similar to those used in the correlation function evaluation indicated that the extrapolated regions only contribute <10% of the total invariant. In spite of these complications and the inherent complex morphology, the "pseudo-two-phase" model with no adjustable parameter nicely reproduces the composition dependence and adequately predicts the absolute magnitude of the invariant.

Figure 13 shows a series of correlation functions for the AP blends. Direct quantitative interpretation of the correlation function results is complicated by the presence of PCL and PC lamellae. However, it it still instructive to examine the detailed morphological features of the composite lamellae. The long period calculated directly from SAXS and that derived from the correlation function were in good agreement as shown in Figure 14. This correlation analysis indicates that both the crystal-phase and amorphous-phase thicknesses were almost independent of the PC composition. This finding could suggest that the PCL lamellae were not significantly perturbed by the addition of PC assuming that the lamellar scattering observed in the semicrystalline/semicrystalline state predominantly came from the PCL lamellae. This ap-

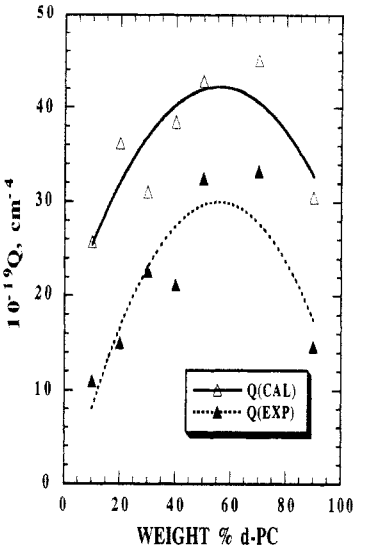

Figure 15. Comparison of the experimentally measured absolute invariant (EXP) to the calculated invariant (CAL) in the semicrystalline/amorphous state.

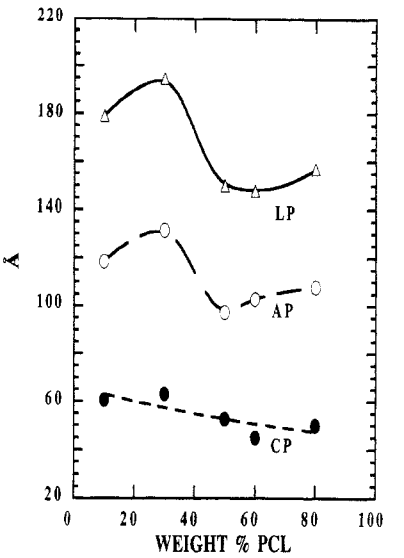

Figure 16. Correlation function results for d-PC/PCL blends in the semicrystalline/amorphous state. LP = PC long period, CP = PC crystalline-phase thickness, and AP = PC amorphous-phase thickness.

proximation is only valid for samples with low PC crystallinties.

III. Structure of Semicrystalline/Amorphous Blends. Measurements were also performed at 75 °C to render the PCL amorphous. Since the SAXS patterns arise only from PC lamellar scattering, the interpretation is more straightforward. Focus can be directed at a more critical examination of the PC lamellar organization in the semicrystalline/amorphous state. Figure 8 shows the long period as a function of PC composition for both the AP and Q blends. Due to annealing effects, the PC long periods for the AP blends were always larger than those for the Q blends. The PC long period for the blends was fairly independent of composition and was larger than the pure PC long period. This difference may be related to the disparity in the thermodynamic driving force for crystallization between the blends and the pure PC. Due to the plasticization of PC by PCL, the T_g of the blend was much lower than that of the pure PC as illustrated in Figure 1. This large depression in T_g indicates that PCL was a very effective macromolecular plasticizer for PC.

Similarly, the peak width for the AP blends was smaller than that for the Q blends, reflecting a more homogeneous lamellar distribution resulting from annealing. Broadening of the lamellar peak increased with increasing PCL as shown in Figure 9. As more PCL was incorporated in the blends, heterogeneity in the PC lamellar sizes increased, leading to a broadening of the lamellar peak. Moreover, Porod analysis indicates that the interfacial thickness was smaller than that found in the semicrystalline/semicrystalline state and increased with increasing PC. Incorporation of PCL in the blends resulted in a reduction of the interfacial thickness relative to the pure PC. Combination of the Porod results derived from the two states demonstrates that the interfacial thickness is strongly affected by both the physical state and the composition of the respective components.

As in the semicrystalline/semicrystalline case, the invariant was calculated by

$$Q = 2\pi^2[\phi_1\phi_2(\rho_1 - \rho_2)^2 + \phi_1\phi_3(\rho_1 - \rho_3)^2 + \phi_2\phi_3(\rho_2 - \rho_3)^2] \quad (7)$$

where subscript 1 denotes crystalline PC, subscript 2 amorphous PC, and subscript 3 amorphous PCL phase. The measured invariant and the calculated value are plotted in Figure 15. In spite of the simplicity of this model, the calculation accurately reproduces the composition dependence of the experimentally obtained invariant. As in the case of the semicrystalline/semicrystalline blends, the calculated values were roughly 50% larger than the measured values. This disparity may be attributed to reasons described earlier.

As discussed earlier, correlation function analysis provides very localized morphological information regarding the organization of the lamellae. The interlamellar spacing, crystal-phase thickness, and amorphous-phase thickness for the solution-cast (d-PC/PCL) blends are shown in Figure 16. For the PCL-rich blends, the long period and the associated morphological parameters were almost independent of composition. The invariance of the amorphous-phase thickness with composition indicated that PCL was rejected from the interlamellar region. In contrast, the amorphous-phase thickness for the PC-rich blends increased with increasing PC whereas the crystal-phase thickness remained fairly constant. This phenomenon suggests that PCL was incorporated or trapped within the interlamellar region, resulting in an increase in the amorphous-phase thickness.

The transition between interlamellar exclusion and interlamellar inclusion of PCL in the PC lamellae may be related to the glass transition temperatures of the blends. For the PCL-rich blends, the T_g was below room temperature, and therefore the chains were highly mobile at the crystallization temperatures of PC. Under these conditions, PCL can readily diffuse away from the growing crystal front and consequently was excluded from the interlamellar region of the PC lamellae. In the case of PC-rich blends, the T_g was above room temperature and the PCL mobility was highly hindered at room temperature and even at the drying temperature (90 °C). Therefore, the mode of incorporation or exclusion is controlled by a competition between entropy and mobility or diffusion. As evidenced by the SAXS results, PCL was trapped within the interlamellar region of the PC lamellae, which led to a corresponding increase in the long period. This increase was attributed to the incorporation of PCL in the amorphous region of the d-PC lamellae.

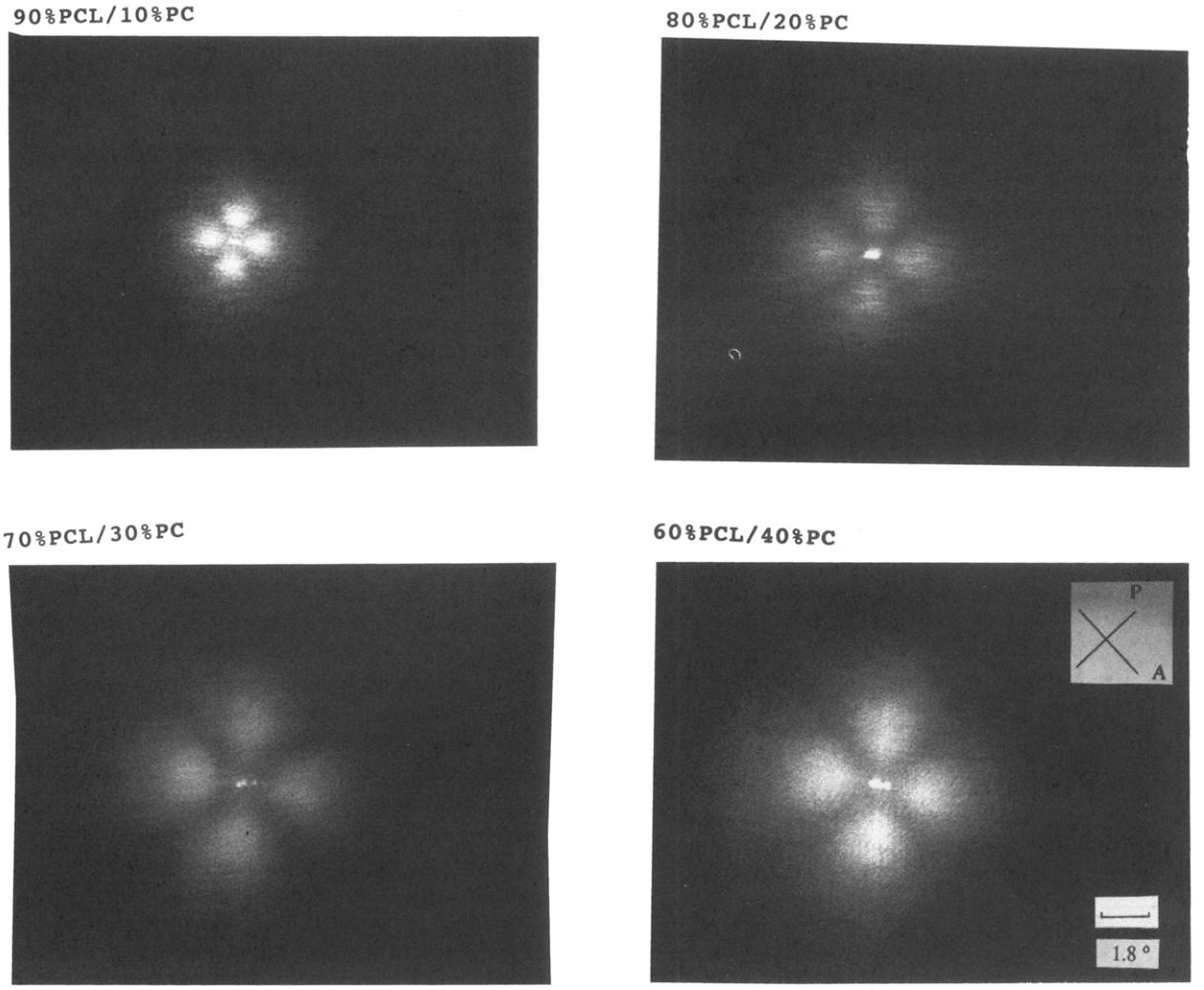

Figure 17. Small-angle light scattering (SALS) patterns for PCL-rich blends recorded at room temperature.

Interlamellar exclusion is always entropically favorable provided the amorphous component has sufficient mobility to diffuse away from the crystalline lamellae. However, interlamellar inclusion occurs when either the amorphous component is highly immobile or the specific interactions are so favorable that the enthalpic term dominates the entropy contribution. On the basis of this finding, the driving force governing the transition from interlamellar exclusion to interlamellar inclusion is controlled by entropy and mobility as is seen in the correlation function results.

Small-Angle Light Scattering. SALS and optical microscopy are most suitable for probing the spherulitic structure of semicrystalline polymers. The SALS H_v patterns for the PCL-rich blends recorded at room temperature are shown in Figure 17. The scattering patterns become larger with increasing PC incorporation. This simply indicates that the PCL spherulitic size decreased with increased PC due to the inverse relationship between the reciprocal space observed with SALS and the real space.[30] In agreement with the crystallization kinetics studies,[31,32] PC was found to be a very effective nucleating agent for PCL crystallization. This nucleating effect results in an acceleration of the PCL crystallization kinetics and a reduction in the PCL spherulitic size with the addition of PC. At temperatures above the melting point of PCL, the sample appeared nearly dark under cross-polarization conditions, suggesting that the PC crystals and crystallinity were too small to be imaged by either SALS or microscopy.

Summary

The lamellar organization of the semicrystalline/semicrystalline and semicrystalline/amorphous PCL/PC blends was investigated with SAXS. Quantitative SAXS analysis was performed to obtain morphological parameters including the interlamellar spacing, peak width at half-height, amorphous- and crystal-phase thicknesses, interfacial width, and the invariant. In the semicrystalline/semicrystalline state, a model based on the random mixing of PCL and PC lamellae provided a rational explanation for the composition dependence of the long period and the peak width at half-height. The SAXS profiles were interpreted in terms of scattering from entities composed of a random mixture of PCL and PC lamellae.

In the semicrystalline/amorphous state (above the melting point of PCL) two distinct regions of incorporation were observed. In the case of PCL-rich blends, PCL was rejected from the interlamellar region of the PC lamellae as indicated by the invariant of the long period and the amorphous-phase thickness. In the case of PC-rich blends, PCL was incorporated between the crystalline PC lamellae as supported by the increases in the amorphous-phase thickness with the addition of PCL. This transition from interlamellar exclusion to interlamellar inclusion was postulated to be related to the glass transition temperatures or the mobility of the blends. Hence, it is seen that the mode of incorporation or exclusion is governed by the competition between entropy and diffusion or mobility. Interlamellar exclusion is always entropically favorable provided the amorphous component has sufficient mobility

to diffuse away from the crytalline lamellae. It is observed that interlamellar exclusion found in the PCL-rich blends is entropy-controlled whereas interlamellar inclusion found in the PC-rich blends is mobility-controlled. SALS coupled with optical microscopy indicated that the PCL spherulitic size decreased with the addition of PC. In agreement with the crystallization kinetics studies,[31,32] PC was found to be an effective nucleating agent for PCL crystallization.

Acknowledgment. This research is supported by Novacor Inc. and also in part by the Division of Materials Sciences, U.S. Department of Energy, under Contract No. DE-AC05-84OR21400 with Martin Marietta Energy Systems, Inc. The authors thank H. E. Yang and P. Yazobucci of Eastman Kodak Co. for the deuterated polycarbonate synthesis.

References and Notes

(1) Cheung, Y. W.; Stein, R. S. *Macromolecules*, preceding paper in this issue.
(2) Bittiger, H.; Marchessault, R. H. *Acta Crystallogr.* **1970**, *B26*, 1923.
(3) Bonart, V. A. *Makromol. Chem.* **1966**, *92*, 146.
(4) Cruz, C. A.; Paul, D. R.; Barlow, J. W. *J. Appl. Polym. Sci.* **1979**, *23*, 589.
(5) Jonza, J. M.; Porter, R. S. *Macromolecules* **1986**, *19*, 1946.
(6) Cheung, Y. W.; Stein, R. S.; Wignall, G. D.; Yang, H. E. *Macromolecules* **1993**, *26*, 5365.
(7) Russell, T. P.; Stein, R. S. *J. Polym. Sci., Polym. Phys. Ed.* **1983**, *21*, 999.
(8) Morra, B. S. *Ph.D. Thesis*, University of Massachusetts at Amherst, MA, 1980.
(9) Russell, T. P.; Ito, H.; Wignall, G. D. *Macromolecules* **1988**, *21*, 1703.
(10) Warner, F. P.; Stein, R. S.; MacKnight, W. J. *J. Polym. Sci., Polym. Phys. Ed.* **1977**, *15*, 2113.
(11) Keith, H. D.; Padden, F. J. *J. Appl. Phys.* **1964**, *35*, 1270, 1286.
(12) Tanaka, H.; Lovinger, A. J. *Macromolecules* **1987**, *20*, 2683.
(13) Tashiro, K.; Satkowski, M. M.; Stein, R. S.; Li, Y.; Chu, B.; Hsu, S. L. *Macromolecules* **1992**, *25*, 1809.
(14) Brandrup, J.; Immergut, E. H. *Polymer Handbook*, 2nd ed.; Wiley: New York, 1975.
(15) Khamatta, F. B.; Warner, F.; Russel, T. P.; Stein, R. S. *J. Polym. Sci., Polym. Phys. Ed.* **1976**, *14*, 1391.
(16) Wignall, G. D.; Lin, J. S.; Spooner, S. J. *J. Appl. Crystallogr.* **1990**, *23*, 241.
(17) Russell, T. P.; Lin, J. S.; Spooner, S.; Wignall, G. D. *J. Appl. Crystallogr.* **1988**, *21*, 629.
(18) Vonk, C. G.; Kortleve, G. *Kolloid Z. Z. Polym.* **1967**, *220*, 19.
(19) Strobl, G. R.; Schneider, M. *J. Polym. Sci., Polym. Phys. Ed.* **1980**, *18*, 1343.
(20) Balta-Calleja, F. J.; Vonk, C. G. *X-Ray Scattering of Synthetic Polymers*; Elsevier: Amsterdam, 1989.
(21) Blundell, D. J. *Acta Crystallogr., Sect. A* **1970**, *26*, 472, 476.
(22) Gerasimov, V. I.; Tsvankin, D. Y. *J. Polym. Sci., Polym. Phys. Ed.* **1974**, *12*, 2035.
(23) Hosemann, R.; Bagchi, S. N. *Direct Analysis of Diffraction by Matter*; North-Holland: Amsterdam, 1962.
(24) Porod, G. *Kolloid-Z.* **1951**, *124* (2), 83.
(25) Porod, G. *Kolloid-Z.* **1952**, *125* (2), 108.
(26) Koberstein, J. T.; Morra, B.; Stein, R. S. *J. Appl. Crystallogr.* **1980**, *13*, 34.
(27) Vonk, C. G. In *Small Angle X-Ray Scattering*; Glatter, O., Kratky, O., Eds.; Academic Press: New York, 1982.
(28) Roe, R. J. *J. Appl. Crystallogr.* **1982**, *15*, 182.
(29) Hahn, B. R.; Herrmann, S.; Wendorff, J. H. *Polymer* **1987**, *28*, 201.
(30) Stein, R. S.; Rhodes, M. B. *J. Appl. Phys.* **1965**, *26*, 3072.
(31) Cheung, Y. W.; Stein, R. S.; Chu, B.; Wu, G. *Macromolecules*, submitted.
(32) Cheung, Y. W.; Stein, R. S., in preparation.